Isorhamnetin Protects Zearalenone-induced Damage via the PI3K/Akt Signaling Pathway in Porcine Granulosa Cells

Xiaoya Li
Northwest A&F University: Northwest Agriculture and Forestry University
Huali Chen
Southwest University of Science and Technology
Zelin Zhang
Northwest A&F University: Northwest Agriculture and Forestry University
Xiaodi Li
Hebei University of Chinese Medicine
Jiaxin Duan
Northwest A&F University: Northwest Agriculture and Forestry University
Rongmao Hua
Northwest A&F University: Northwest Agriculture and Forestry University
Li Yang
Northwest A&F University: Northwest Agriculture and Forestry University
Jianyong Cheng
Northwest A&F University: Northwest Agriculture and Forestry University
Qingwang Li (Liqingwang@nwafu.edu.cn)
Northwest A&F University: Northwest Agriculture and Forestry University https://orcid.org/0000-0001-7176-0320

Research

Keywords: Zearalenone, Isorhamnetin, Ovarian granulosa cells, Apoptosis, Proliferation, PI3K/Akt

Posted Date: October 12th, 2021

DOI: https://doi.org/10.21203/rs.3.rs-960299/v1

Abstract

Background: Zearalenone (ZEA) is widely derived from moldy cereal grain, which has adverse effects on animal reproduction. In particular, pigs are more sensitive to ZEA-induced toxicity than other animals. Isorhamnetin, a flavonoid has extensive of pharmacological activities. However, little is known about the effects of isorhamnetin on reproduction. Thus, it would be interesting to clarify the effect and the underlying molecular mechanism of isorhamnetin involvement in ZEA-induced cytotoxicity in porcine granulosa cells.

Results: Our findings showed that isorhamnetin suppressed ZEA-induced apoptosis by regulating Bcl-2 and Bax protein changes. Changes in intracellular Ca2+ levels and CHOP, ATF6, GRP78 indicated that isorhamnetin rescued ZEA-induced endoplasmic reticulum stress (ERS). Furthermore, isorhamnetin prevented ZEA-induced reactive oxygen species (ROS) via P38 signaling pathway. Mechanistically, isorhamnetin stimulated the expression of PCNA and CyclinD, thereby raising the ratio of S phases cells in response to ZEA-induced apoptosis via PI3K/Akt signaling pathway. Isorhamnetin also recovered ZEA-induced steroidogenesis disorder by regulating steroidogenic enzyme gene and proteins (FSH-R, CYP19A1).

Conclusions: Collectively, these findings show that isorhamnetin protects granulosa cells from ZEA-induced damage via the PI3K/Akt signaling pathway, which promotes proliferation, alleviates steroidogenesis disorder, ERS and oxidative stress.

Introduction

In mammalian ovaries, granulosa cells (GCs) play a vital role in follicular growth, oocyte maturation, ovulation and steroidogenesis [1]. GCs are indispensable for folliculogenesis. Previous report demonstrated that GCs affected follicular development by releasing follicular growth and maturation factors [2]. Moreover, GCs provided nutrients for oocytes and made them have full developmental ability [3, 4]. More than 99% of follicles will undergo atresia in the process of follicular formation. Most follicular atresia is caused by GCs apoptosis [5]. However, ZEA increased GCs apoptosis in a dose-dependent manner, thereby disrupting follicular development [6]. In addition, recent studies have shown that ZEA induced apoptosis in GCs in different species [7, 8]. Further research indicated that excessive ZEA could cause oxidative stress and lead to cytotoxicity [9]. ZEA is commonly found in feeds and food, which can induce to irreversible toxic damage to the development of embryos and the reproductive system. Specifically, pigs are more sensitive to ZEA than other animals. Moreover, ZEA could accumulate in the meat products through the food chain, which might be harmful to humans [10]. Thus, it is of great significance to explore effective methods to alleviate the toxicity of ZEA.

Isorhamnetin, a natural flavonoid, which is widely distributed in fruits and vegetables [11]. In addition, isorhamnetin is a safe, inexpensive and convenient dietary ingredient for women [11].

Isorhamnetin can regulate cardiovascular, prevent obesity, alleviate cell apoptosis and inflammation [11]. However, little is known about the effects of isorhamnetin on reproduction. Moreover, it is unclear whether isorhamnetin can improve the reproductive system of animals, specifically in ZEA-induced GCs damage. Thus, it would be interesting to clarify the effects of isorhamnetin on ZEA-induced apoptosis in GCs.

PI3K/Akt has the functions of regulating cell growth, proliferation, metabolism and survival.

Studies suggested that isorhamnetin played a role in cell apoptosis [12], oxidative stress [13] and inflammation [11] through the PI3K/Akt signaling pathway. Moreover, Whole-transcriptome analysis showed that PI3K/Akt signaling pathway was involved in the toxic effects of ZEA exposure on ceRNA networks in porcine GCs [6]. Thus, it is necessary to investigate the effects of PI3K/Akt and isorhamnetin on ZEA-induced cytotoxicity.

In this study, we hypothesized that isorhamnetin could alleviate the cytotoxicity of GCs induced by ZEA. In addition, we attempted to find the signaling pathway and potential mechanism of isorhamnetin inhibiting ZEA damage. Our findings may extend the value of isorhamnetin to the application of improving reproductive processes in porcine. Moreover, these findings may also benefit human reproduction and health.

Materials And Methods

Chemical

Isorhamnetin (Cat#: N1358) was obtained from ApexBio. ZEA (Cat#: 17924-92-4) was obtained from Sigma. PI3K antagonist LY294002 (Cat#: S1737) and P38 antagonist SB203580 (Cat#: S1863) were purchased from Beyotime. Sodium phenylbutyrate (4-PBA) (Cat#: 1716-12-7) is an endoplasmic reticulum inhibitor obtained from Santa Cruz Biotechnology. The antibodies used in this study were as follows: anti-LC3B (Cat#: 192890) was purchased from Abcam; Anti-β-actin (Cat#: 66009-1-1g) and p62 (18420-1-AP) were purchased from Proteintech; anti-FSHR (Cat#: WL04496), anti-PCNA (Cat#: WL02208), anti-C-myc (Cat#: WL01781), anti-PI3K (Cat#: WL02240), anti-Akt (Cat#: WL0003b), anti-p-Akt (Cat#: WLP001a), anti-Bcl-2 (Cat#: WL01556), anti-PGC1(Cat#: WL02123), anti-Bax (Cat#: WL01637), Cleaved caspase-3 (Cat#: WL01992), anti-SOD2 (Cat#: WL02506), anti-GPx-1 (Cat#: WL02497a), anti-SOD1 (Cat#: WL01846), anti-Caspase12 (Cat#: WL00735), anti-CHOP (Cat#: WL00880), anti-CalcineurinA (Cat#: WL03449), anti-CaMKIIα (Cat#:WL03453) , anti-ATF6 (Cat#:WL02407), anti-IRE1 (Cat#:WL02562), anti-XBP1 (Cat#:WL00708), anti-GRP78 (Cat#:WL03157), anti-P38 (Cat#: WL00764), anti-P-P38 (Cat#: WLP1576), anti-CyclinA (Cat#: WL01841) and anti-CyclinD (Cat#: WL01435a) were purchased from WanleiBio; anti-CYP19A1 (Cat#: ET1703-77) was obtained from Huabio.

Culture and treatment of GCs

A × (B × C) is the breeding system of porcine, A (Duroc) is the terminal male, B (Landrace) is the matriarchal father, and C (Yorkshire) is the matriarchal mother. Pigs are about 7 months. Porcine ovaries

are obtained from a local abattoir. Porcine ovaries are transported to the laboratory within 1 h in 37°C PBS containing penicillin (100 IU/mL) and streptomycin (100 mg/mL). GCs are separated from follicles using syringe. GCs were mixed in DMEM/F12 medium supplemented with1% streptomycin–penicillin and 8% fetal bovine serum (FBS) (Serapro, Germany). GCs were cultured at 37°C in 5% CO2 for 36 to 44 h. After, GCs were cultured with isorhamnetin and ZEA, and incubated for 24 h in DMEM/F12 medium containing transferrin (2.5 mg/mL), 0.5% bovine serum albumin (BSA) (w/v), sodium bicarbonate (10 mM), insulin (50 ng/mL), sodium selenite (5 ng/mL), FSH (0.1 IU/mL), penicillin (100 U/mL), streptomycin (100 mg/mL) and nonessential amino acid mix (1×) [14]. GCs were collected for protein and mRNA extraction. The media was harvested for an ELISA assay.

EdU and CCK-8 evaluates

EdU-488 (Beyotime, China) was used to examine cell proliferation. GCs were treated with EdU 1:1,000 for 5 h incubation. The procedure was based on the manufacturer's descriptions. After EdU incubation, the images were calculated by fluorescence microscope.

Viability of GCs was tested by CCK-8 (Beyotime, China). The 96-well plate was seeded with GCs. After, GCs were mixed with CCK-8 (10 μL) and for 2 h at 37°C. Then, the optical density was determined using a microplate reader.

Quantitative real-time PCR

The RNA of GCs was extracted using Trizol reagent (Takara, JP) based on the manufacturer’s descriptions. The cDNA was synthesized on ice by the PrimeScript TM RT Reagent Kit (Takara, JP). Quantitative real-time PCR was performed using CHAMQ TM SYBR qPCR Master Mix (China, Vazyme) in a 20μL reaction system. The reagent kit procedures were according to the manufacturer’s descriptions. *β-actin* was used as the housekeeping gene. Then, the relative normalized expression was calculated by the 2−ΔΔCT. The primer sequence is displayed in Table 1.

Western blot analysis

The total protein from GCs was extracted with RIPA lysis buffer (Beyotime, China). BCA kit (Beyotime, China) was used to measure protein concentration. The protein (15 to 20 μg) was separated by 10% to 15% SDS-PAGE gel electrophoresis and transferred to nitrocellulose membrane (Millipore, Billerica, MA, USA). After, the membrane was sealed with QuickBlock™ Western (Beyotime). Then, the membrane was incubated with the primary antibodies overnight at 4°C. Cleaning with TBST, the membrane was sealed with secondary antibodies at room temperature for 1 h. The protein band was detected by X-ray and band intensity was quantified using ImageJ software.

Flow cytometry assay

GCs were treatd by the Cell Cycle Kit (Solarbio, China). GCs were fixed in 75% ethanol at 4°C for overnight. Then, GCs were mixed with PI for 30 minutes at 37°C. Subsequently, GCs were tested using flow

cytometry. ModFit software was used to analyze data.

Detection of ROS and Steroid Hormones Secretion

GCs were treated with fluorescent dye 20,70-dichlorodihydroflorodihyd-rofluorescein diacetate DCFH-DA (Beyotime, China) at 37°C for 20 minutes. Then, GCs were washed 3 times with phosphate buffered saline (PBS). GCs were detected by fluorescence microscope.

The dosage of estrogen (E2) in the medium was determined by a competitive ELISA kit (Ruixin Biotech, China). The detection range of the kit was 40 to 2,000 pg/mL. The lowest value detected was 40 pg/mL. The specific testing steps were carried out according to the instructions.

Measurement of Ca2+ level

Fura-2 AM (Beyotime) was used to detect intracellular Ca2+ content. GCs were mixed with Fura-2 AM (5 μM) for 30 minutes at 37°C. Microplate reader was used to test data.

Measurement of MDA production and Antioxidant enzyme activity

Superoxide Dismutase (SOD) assay kit, Malondialdehyde (MDA) assay kit and Glutathione Peroxidase (GSH-PX) assay kit were bought from Nanjing Jiancheng Bioengineering Institute. The GSH-PX, SOD and MDA were performed according to assay kit descriptions. Briefly, GCs lysates were mixed with detection reagent. Data was analyzed by microplate reader.

Statistical analysis

Data were analyzed with SPSS 18.0 and Graphpad Prism 6. ANOVA and Duncan test were to used compare data. Data were reported as average ±SEM of at least three times. The $P < 0.05$ represented statistical significance.

Results

Isorhamnetin suppressed ZEA-induced apoptosis in GCs

To investigate whether ZEA exposure affects GCs growth and apoptosis. GCs were treated with ZEA (0, 10, 30, 60, 90 and 120 μM) for 24 h. The result indicated that the half maximal inhibitory concentration values of ZEA was 60 μM ($P < 0.05$ Fig. 1B). Pretreatment with isorhamnetin at dosage of 1, 5, 10, 20 and 30 μM increased the cell viability of GCs exposed to 60 μM ZEA for 24 h (Fig. 1C). Interestingly, 20 μM isorhamnetin was the most effective in resisting cytotoxicity ($P < 0.05$; Fig. 1C). Thus, the dosage of 60 μM ZEA and 20 μM isorhamnetin were used in this study. Subsequently, western blot analysis found that Bax and C-Casp3 were increased in ZEA-treated group ($P < 0.05$), whereas the Bcl-2 was decreased ($P < 0.01$; Fig. 1D, E, F, and G). However, isorhamnetin pretreatment could inhibit the changes of Pro-apoptotic proteins (Fig. 1D, E, F, and G). we next detected the mitochondrial quantity using Mito-Tracker Red CMXRos. As shown in Figure 1H, ZEA-exposed GCs showed decreased mitochondrial mass, as seen in

the decline of the Mito-Tracker Red CMXRos fluorescence signals. Conversely, ZEA-induced mitochondrial impairment was partially attenuated by isorhamnetin pretreatment (Figure 1H). Similarly, the western blot analysis revealed a lower protein expression of PGC-1 in ZEA-treated GCs ($P < 0.05$; Fig. 1I, and J). This effect was recovered by isorhamnetin pretreatment (Fig. 1I, and J). Furthermore, ZEA treatment significantly increased the protein expression of LC3II and P62 in GCs, while isorhamnetin therapy effectively relieved this ZEA-induced upregulation ($P < 0.05$; Fig. 1K, L and M). Overall, these findings suggest that isorhamnetin can inhibit GCs apoptosis induced by ZEA.

Isorhamnetin relieved ZEA-induced ERS

Given that ERS could induce apoptosis. We next studied the changes of ERS-related apoptotic markers in GCs. As expected, the protein expression of Casp12 and CHOP were significantly increased in ZEA-treated GCs ($P < 0.05$), which was abolished by isorhamnetin treatment (Fig. 2A, B, and C). In line with this, ZEA treatment alone clearly increased the protein expression of ATF6, IRE1, XBP1 and GRP78 ($P < 0.05$), suggesting that ERS happened in ZEA-exposed GCs (Fig. 2F, G, H, I, and J). But, 4-PBA effectively reduced the protein expression of ATF6, IRE1, XBP1 and GRP78 in ZEA-treated GCs (Fig. 2F, G, H, I, and J). Consistent with the effect of 4-PBA, the changes in ERS proteins could be restored by isorhamnetin treatment (Fig. 2F, G, H, I, and J). Subsequently, We also found that the protein expression of CalcineurinA and CaMKIIα were significantly increased in ZEA-treated GCs ($P < 0.05$), which was then recovered by isorhamnetin treatment (Fig. 2A, D, and E). Interestingly, pretreatment with isorhamnetin or 4-PBA clearly recovered the level of Ca2+ in GCs exposed to ZEA ($P < 0.01$; Fig. 2K). The data show that isorhamnetin can block ZEA-induced ERS and maintains ER homeostasis.

Isorhamnetin relieved oxidative stress caused by ZEA

High levels of ROS also lead to GCs apoptosis. We next measured P-P38 signals in the ZEA- treated GCs, which was believed to be engaged in antioxidative stress. Western blot analysis indicated that an effective activation of P-P38 signaling occured in the ZEA-treated GCs (($P = 0.03$; Fig. 3A, and E). Furthermore, the protein expression of SOD2, GPX1 and SOD1 were decreased in ZEA-treated GCs, which was partially recovered by isorhamnetin treatment ($P < 0.05$; Fig. 3A, B, C, and D). Additionally, the content of MDA was increased, whereas the activities of SOD and GSH-PX were decreased in ZEA-treated GCs ($P < 0.05$; Fig. 3F, G, and H). However, ZEA-induced damage was relieved by isorhamnetin therapy ($P < 0.05$; Fig. 3A, B, C, D, E, F, G, and H). Interestingly, SB203580, P38 MAPK antagonist, blocked ZEA-inhibited the protein expression of SOD2 and GPX1 in GCs, which was partially mimicked by isorhamnetin ($P < 0.05$; Fig. 3K, L, and M). Furthermore, ZEA increased the level of ROS in GCs, and isorhamnetin inhibited ROS accumulation via its antioxidant activity ($P = 0.003$; Fig. 3I, and J). Similarly, the ROS generation induced by ZEA treatment was partially alleviated when the GCs were treated with SB203580 (Fig. 3I, and J). These data indicate that isorhamnetin can inhibit ROS in GCs induced by ZEA via down-regulating the P-P38/P38.

Isorhamnetin recovered GCs proliferation caused by ZEA through the PI3K/Akt signaling pathway

We further investigated how isorhamnetin alleviated the loss of GCs caused by ZEA. ZEA treatment decreased the protein expression of PCNA, C-myc, PI3K and P-Akt/Akt in GCs ($P < 0.05$; Fig. 4A, B, C, D, and E). This action was recovered by isorhamnetin therapy (Fig. 4A, B, C, D, and E). In line with this, the proliferation of GCs treated with ZEA was significantly inhibited by Edu staining, which was alleviated by isorhamnetin ($P = 0.007$; Fig. 4F, and G); this beneficial action was abolished by LY294002 (Fig. 4F, and G). Subsequently, we found that a marked decrease in the protein expression of CyclinD and CyclinA in ZEA-treated GCs ($P < 0.05$; Fig. 4H, I, and J). However, co-treatment with isorhamnetin significantly increased the expression of cycle-related proteins in GCs (Fig. 4H, I, and J). Similarly, flow cytometry data showed that ZEA treatment improved the ratio of cells in the G0/G1 phase, whereas the ratio of cells in the S phases was decreased ($P = 0.003$; Fig. 4K, L, M, and N). However, the decrease of S phase cells was inhibited when GCs were treated with isorhamnetin ($P = 0.003$; Fig. 4K, L, M, and N). Furthermore, isorhamnetin-induced cell division was abolished by LY294002 (Fig. 4K, L, M, and N). The data indicate that isorhamnetin depends on the PI3K/Akt signaling pathway, which recovers GCs proliferation in response to ZEA-stimulated apoptosis.

Isorhamnetin prevented ZEA-induced steroid secretion disorder in a PI3K/Akt-dependent manner

To explore the effect of isorhamnetin on GCs steroidogenesis in response to ZEA treatment, we next measured the indicators related to hormone secretion. Western blot analysis showed ZEA treatment decreased the protein expression of FSH-R and CYP19A1 in GCs ($P < 0.05$; Fig. 5A, B, and C). This action was recovered by isorhamnetin pretreatment (Fig. 5A, B, and C). Similarly, ZEA-treated GCs significantly inhibited the mRNA expression of *CYP19A1*, *FSH-R*, *ER2* and *ER1*, which was restored by isorhamnetin administration ($P < 0.05$; Fig. 5E, F, G, and H). However, isorhamnetin increased the secretion of E2 in GCs, which was abolished by LY294002 ($P = 0.007$; Fig. 5D). The secretion of E2 in GCs was consistent with the expression trend of E2-synthesized mRNA (Fig. 5D, E, F, G, and H). These results suggest that isorhamnetin alleviates ZEA-induced steroid secretion disorder through the PI3K/Akt.

Discussion

ZEA is widely found in moldy cereal grain, which is harmful to the growth of gametogenesis and embryo in animals and human [10]. ZEA can cause poisoning to animals and damage the reproductive system of animals [15]. In particular, pigs are more sensitive to ZEA than other animals. Thus, it is of great significance to explore effective methods to alleviate the toxicity of ZEA to porcine GCs. Isorhamnetin, a flavonoid compound, has a wide range of pharmacological effects, including anti-oxidation, anti-inflammation, anti-bacterial, anti-virus and anti-tumor [16]. However, it's still uncertain whether isorhamnetin attenuates ZEA-induced damage in GCs. Here, our research showed that isorhamnetin inhibited the apoptosis of GCs caused by ZEA. In addition, this study indicated that isorhamnetin alleviated ZEA-induced GCs damage via the PI3K/Akt.

To elucidate the beneficial mechanism of isorhamnetin on ZEA-induced apoptosis, GCs were utilized. The Bcl-2 family regulates the cytochrome c release and thereby starts the caspase cascade, a well-known

apoptotic pathway [17]. Published data have suggested that 60 μM ZEA could significantly reduce the cells viability of mouse ovarian GCs and induce apoptosis [18]. Consistently, we found that ZEA activated the protein expression of Bax and C-Casp3 in GCs. However, isorhamnetin could rescue mitochondrial apoptosis induced by ZEA. Indeed, isorhamnetin could inhibit caspase-3 in H_2O_2-treated PC12 cells [19]. Moreover, isorhamnetin has a protective effect on endothelial cell apoptosis caused by oxidized low-density lipoprotein [20]. Mitochondrial dysfunction has been considered as a major factor inducing cell death [21]. Strong evidence indicated that ZEA could influence mitochondrial functions [22]. Previous study confirmed that ZEA caused the loss of mitochondrial transmembrane potential in porcine GCs [23]. Similarly, we found that isorhamnetin could recover the expression of PGC-1 to alleviate the mitochondrial dysfunction caused by ZEA. Furthermore, isorhamnetin alleviated the autophagy of GCs in the presence of ZEA. Indeed, isorhamnetin has been reported to prevent autophagy in response to apoptosis in mice [24]. It is thus conceivable that isorhamnetin rescues the ZEA damage by regulating apoptosis, autophagy and mitochondrial function of GCs Bcl-2 protein.

When the ER function is badly impaired, the expression of ERS related markers and the organelles changes, which leads to apoptosis [25]. Our data showed that isorhamnetin decreased the expression of Casp12 and CHOP, which were associated with ERS. Subsequently, the changes of ER membrane sensors-related proteins ATF6, IRE1, XBP1 and GRP78 showed that isorhamnetin relieved ZEA-induced ERS. Similarly, previous study confirmed that isorhamnetin inhibited collagen deposition in N2a cells by alleviating ERS [26]. ERS could disturb the balance of Ca2+ [27]. Research have shown that isorhamnetin inhibited Ca2+ overload and alleviated ERS-induced apoptosis in N2a cells [26]. In addition, pretreatment with isorhamnetin could directly decrease the level of Ca2+ in H_2O_2-treated PC12 cells [19]. Consistently, we found that isorhamnetin alleviated the increase of Ca2+ in ZEA-induced GCs by reducing the protein expression of calcineurinA and CaMKIIα. Our data show that isorhamnetin may alleviate ZEA-induced GCs apoptosis by inhibiting ERS.

Study indicated that oxidative stress and ERS, as closely related events, played a vital role in cellular apoptosis [27]. Studies showed that ZEA could cause oxidative stress in human cells and mouse sertoli cells [28, 29]. Likewise, Pan et al [30] reported that ZEA stimulated MDA level and inhibited the expression of Sod2, Sod1, Cat and Gpx1 in rat placenta through mTOR signaling pathway. In our study, ZEA also stimulated MDA level and decreased the protein expression of SOD2, GPX1 and SOD1 by activating P-P38 pathway. Fortunately, isorhamnetin played a beneficial role in response to ZEA-induced oxidative stress. Similarly, previous research shown that isorhamnetin inhibited the content of MDA and increased the activity of SOD and GSH-Px activity in APAP-induced injured 102 cells [31]. Strong evidence indicated that isorhamnetin suppressed P-P38 to against oxidative stress in PC12 Cells [19]. Furthermore, isorhamnetin could inhibit ConA-induced autophagy and apoptosis via the P38/PPAR-α pathway in mice [24]. These data show that isorhamnetin can against ZEA-induced oxidative stress through the P-P38 signaling pathways.

Cell cycle progression is a vital physiological process in cell life activities, and interference with cell cycle often leads to aging, degeneration or apoptosis [32]. The changes of cell cycle related proteins is crucial

in regulating cell cycle progression [33]. Research have shown that ZEA regulated the expression of CyclinB and CyclinD proteins, leading disruption of the cell cycle and reducing cell viability [34]. Recent study provided evidence that the cell cycle of ZEA-treated porcine GCs was arrested in the G2/M phase [6]. Interestingly, we found that the S phase of DNA synthesis was decreased in ZEA-treated GCs. Furthermore, ZEA inhibited CyclinA and CyclinD in GCs, which was consistent with the results of flow cytometry analysis. Jiang found that isorhamnetin blocked cells from entering S phase of DNA synthesis, and finally inhibited the proliferation of HepG-2 cells [35]. On the contrary, our data showed that isorhamnetin stimulated CyclinD and PCNA, and the proportion of EdU positive cells, which recovered GCs proliferation in response to ZEA-stimulated apoptosis. Subsequently, isorhamnetin increased the S phase of DNA synthesis in GCs, which was suppressed by the PI3K/Akt inhibitor. These data suggest that isorhamnetin restores GCs proliferation against ZEA-induced apoptosis and subsequently increases the S phase of DNA synthesis via the PI3K/Akt.

Healthy follicles have higher concentrations of E2 [14, 36]. Thus, the steroidogenesis of GCs is essential for atresia and follicular development. Growing evidence has revealed that ZEA altered the production of steroid hormones in GCs [23, 37]. In vitro studies suggested that ZEA (20 mg/kg) reduced the concentration of E2 in serum of pregnant rats [38]. Dietary supplementation of ZEA reduced serum E2 level in female pigs [39]. Similarly, our data demonstrated that ZEA suppressed E2 secretion of GCs. However, this action was recovered by isorhamnetin pretreatment. Strong evidence has shown that hormone synthesis was controlled by steroidogenic enzymes, including CYP19A1 and hormone receptor [40]. Recent studies demonstrated that the protein expression of CYP19A1 was an important enzyme for E2 biosynthesis [41]. Consistently, Our observations showed that isorhamnetin regulated the expression of steroid-related genes and proteins to alleviate the hormone balance disturbed by ZEA-treated GCs. Furthermore, our data also showed that the protective actions of isorhamnetin on ZEA-induced hormonal disorders was abolished by PI3K inactivation. Indeed, isorhamnetin has a possible protective action inhibit oxidative stress in human RPE cells by activating the PI3K/Akt signaling pathway [13]. In brief, isorhamnetin recovered ZEA-induced steroid secretion disorder through PI3K/Akt activation.

Conclusion

In conclusion, we found that a novel role of isorhamnetin in alleviating the damage caused by ZEA in GCs. We first demonstrated that isorhamnetin protected GCs from ZEA-induced damage via the PI3K/Akt, which recovered the proliferation and E2 secretion of GCs. Additionally, isorhamnetin prevented ZEA-induced oxidative stress and ERS in a P-P38-dependent manner. These data indicate that isorhamnetin can effectively reduce the damage caused by ZEA in porcine GCs, which shows great promise for applications of isorhamnetin in alleviating ZEA-associated reproductive toxicity. Thus, humans and animals will be healthier, and food and feed products can be protected.

Abbreviations

ZEA: Zearalenone; ERS: endoplasmic reticulum stress; ROS: reactive oxygen species; GCs: Granulosa cells; FBS: Fetal bovine serum; BSA: Bovine serum albumin; PBS: phosphate buffered saline; SOD: Superoxide Dismutase; MDA: Malondialdehyde; GSH-PX: Glutathione Peroxidase; E2: estrogen.

Declarations

Acknowledgments

Not applicable.

Authors' contributions

X. Li produced the initial draft of the manuscript and carried out experiments and analyzed the data. H.Chen., Z.Zhang., and J. Duan. helped to design the entire research concept. R. Hua,. and X. Li . helped with ovarian preparation and GCs cultivation. L.Yang., and J. Cheng .assisted in conducting experiments. Q. Li. revised the manuscript. All authors read and approved the final manuscript. All authors read and contributed to the manuscript.

Funding

This study was financially supported by Ministry of Agriculture Transgenic Major Projects (2018ZX0801013B) and Key Industry Innovation Chain of Shaanxi Province (2018ZDCXL-NY-02-06).

Availability of data and materials

The datasets used and/or analyzed during the current study are available from the corresponding author on request.

Ethics approval and consent to participate

All animal care and procedures were performed in accordance with institutional and national guidelines and approved by the the Utilization Committee of Northwest A&F University (Yangling, China).

Consent for publication

Not applicable.

Competing interests

The authors declare no competing financial interest.

References

1. Guler S, Zik B. Effects of capsaicin on ovarian granulosa cell proliferation and apoptosis. *Cell Tissue Res*. 2018;372:603-609.

2. Lai F, Liu J, Li L, Ma J, Liu X, Liu Y, et al. Di (2-ethylhexyl) phthalate impairs steroidogenesis in ovarian follicular cells of prepuberal mice. *Arch Toxicol*. 2017;91: 1279-1292.
3. Jiang J, Xiong H, Cao M, Xia X, Sirard M, Tsang B. Mural granulosa cell gene expression associated with oocyte developmental competence. J. Ovarian. Res. 2010;3:1-12.
4. Sugiura K, Pendola F, Eppig J. Oocyte control of metabolic cooperativity between oocytes and companion granulosa cells: energy metabolism. Dev. Biol. 2005;279:20-30.
5. Inoue N, Matsuda F, Goto Y, Manabe N. Role of cell-death ligand-receptor system of granulosa cells in selective follicular atresia in porcine ovary. J. Reprod. Develop. 2011;57:169-175.
6. Li N, Liu X, Zhang F, Tian Y, Zhu M, Meng L, et al. Whole-transcriptome analysis of the toxic effects of zearalenone exposure on ceRNA networks in porcine granulosa cells. Environ Pollut. 2020;261:114007.
7. Zhang R, Sun X, Wu R, Cheng S, Zhang G, Zhai Q, et al. Zearalenone exposure elevated the expression of tumorigenesis genes in mouse ovarian granulosa cells. Tpxicol Appl Pharmacol. 2018;356:191-203.
8. Liu X, Wu R, Sun X, Cheng S, Zhang R, Zhang T, et al. Mycotoxin zearalenone exposure impairs genomic stability of swine follicular granulosa cells in vitro. Int. J.Bio. Sci. 2018;14:294-305.
9. Long M, Yang S, Wang Y, Li P, Zhang Y, Dong S, et al. The Protective Effect of Selenium on Chronic Zearalenone-Induced Reproductive System Damage in Male Mice. Molecules. 2016;21: 1687.
10. Yang D, Jiang X, Sun J, Li X, Li X, Jiao R, et al. Toxic effects of zearalenone on gametogenesis and embryonic development: A molecular point of review. Food Chem Toxicol. 2018;119:24-30.
11. Gong G, Guan Y, Zhang Z, Rahman K, Wang S, Zhou S, et al. Isorhamnetin: A review of pharmacological effects. Biomed Pharmacother. 2020;128:110301.
12. Gao L, Liu Y, Wang Z, Huang Z, Du B, Zhang D, et al. Isorhamnetin protects against cardiac hypertrophy through blocking PI3K-AKT pathway. Mol. Cell. Biochem. 2017;429:167-177.
13. Wang J, Gong H, Zou H, Wu X. Isorhamnetin prevents H2O2-induced oxidative stress in human retinal pigment epithelial cells. Mol. Med. Rep. 2018;17:648-652.
14. Chen H, Yang Y, Wang Y, Li Y, He Y, Duan J, et al. Phospholipase c inhibits apoptosis of porcine primary granulosa cells cultured in vitro. J. Ovarian. Res. 2019;12:90.
15. Zhao F, Li R, Xiao S, Diao H, Viveiros M, Song X, et al. Postweaning exposure to dietary zearalenone, a mycotoxin, promotes premature onset of puberty and disrupts early pregnancy events in female mice. Toxicol Sci. 2013;132:431-442.
16. Teng D, Luan X. Research progress of isorhamnetin in pharma codynamics. Clin.J. Tradit. Chin. Med. 2016;28:593-596.
17. Woo M, Noh J, Cho E, Song Y. Bioactive Compounds of Kimchi Inhibit Apoptosis by Attenuating Endoplasmic Reticulum Stress in the Brain of Amyloid β-Injected Mice. J. Agric. Food Chem. 2018;66:4883-4890.

18. Yi Y, Wan S, Hou Y, Cheng J, Guo J, Wang S, et al. Chlorogenic acid rescues zearalenone induced injury to mouse ovarian granulosa cells. Ecotoxicol. Environ. Saf. 2020;194:110401.
19. Hwang S, Yen G. Modulation of Akt, JNK, and p38 activation is involved in citrus flavonoid-mediated cytoprotection of PC12 cells challenged by hydrogen peroxide. J. Agric. Food Chem. 2009;57:2576-2582.
20. Bao M, Xiao Y, Leng Y. The protective effects of isorhamnetin on endothelial cell apoptosisi induced by oxidized low density lipoprotein. Chin. j . Atherbladder. 2010;18:445-448.
21. Marra F, Svegliati-Baroni G. Lipotoxicity and the gut-liver axis in NASH pathogenesis. J HEPATOL. 2018;68:280-295.
22. Razi, Mazdak, Malekinejad, Hassan, Adibnia, Elmira. Zearalenone and 17 β-estradiol induced damages in male rats reproduction potential; evidence for ERα and ERβ receptors expression and steroidogenesis. Toxicon. 2016;120:133-146.
23. Zhu L, Yuan H, Guo C, Lu Y, Deng S, Yang Y, et al. Zearalenone induces apoptosis and necrosis in porcine granulosa cells via a caspase-3- and caspase-9-dependent mitochondrial signaling pathway. J. Cell. Physiol. 2012;227:1814-1820.
24. Lu X, Liu T, Chen K, Xia Y, Dai W, Xu S, et al. Isorhamnetin: A hepatoprotective flavonoid inhibits apoptosis and autophagy via P38/PPAR-α pathway in mice. Biomed. Pharmacother. 2018;103:800-811.
25. Li Y, Guo Y, Tang J, Jiang J, Chen Z. New insights into the roles of CHOP-induced apoptosis in ER stress. Acta. Biochim. Biophys. 2014;46: 629-640.
26. Qiu L, Ma Y, Luo Y, Cao Z, Lu H. Protective effects of isorhamnetin on N2a cell against endoplasmic reticulum stress-induced injury is mediated by PKCε. Biomed Pharmacother. 2017; 93:830-836.
27. Xu D, Liu L, Zhao Y, Yang L, Cheng J Hua R, et al. Melatonin protects mouse testes from palmitic acid-induced lipotoxicity by attenuating oxidative stress and DNA damage in a SIRT1-dependent manner. J Pineal Res. 2020;69:e12690.
28. Zheng W, Wang, B, Wang L, Shan Y, Zou H, Song R, et al. ROS-Mediated Cell Cycle Arrest and Apoptosis Induced by Zearalenone in Mouse Sertoli Cells via ER Stress and the ATP/AMPK Pathway. Toxins. 2018;10:3-16.
29. Tatay E, Espín S, García-Fernández A, Ruiz M. Oxidative damage and disturbance of antioxidant capacity by zearalenone and its metabolites in human cells. Toxiclol. In. Vitro. 2017;45:334-339.
30. Pan P, Ying Y, Ma F, Zou C, Yu Y, Li Y, et al. Zearalenone disrupts the placental function of rats: A possible mechanism causing intrauterine growth restriction. Food. Chem Toxicol. 2020;145:111698.
31. Jiang Z, Wang X, Wang J, Chen X, Wang J, Pan J. Effect of sediherba total flavanones and isorhamnetin on APAP-induced injured l02 cells. Chin. J, Exp, Tradit. Med. 2018;24:121-125.
32. Pack L, Daigh L, Meyer T. Putting the brakes on the cell cycle: mechanisms of cellular growth arrest. Curr. Opin. Cell Biol. 2019;60:106-113.

33. Lim S, Kaldis P. Cdks, cyclins and CKIs: roles beyond cell cycle regulation. Development. 2013;140:3079-3093.
34. Zhang G, Song J, Zhou Y, Zhang R, Cheng S, Sun, X, et al. Differentiation of sow and mouse ovarian granulosa cells exposed to zearalenone in vitro using RNA-seq gene expression. Toxicol. Appl. Pharmacol. 2018;350:78-90.
35. Jiang C, Xiang Y, Zhong Y. Effects of isorhamnetin on the proliferous cycle andapoptosis of human hepatoma HepG-2 cells: an experimental study. J. Milit. Surg. 2012;14:432-435.
36. He Y, Deng H, Jiang Z, Li Q, Shi M, Chen, H, et al. Effects of melatoninon follicular atresia and granulosa cell apoptosis in the porcine. Mol. Reprod. Dev. 2016;83:692-700.
37. Zhang G, Zhang R, Sun X, Cheng S, Wang Y, Ji C, et al. RNA-seq based gene expression analysis of ovarian granulosa cells exposed to zearalenone in vitro: significance to steroidogenesis. Oncotarget. 2017;8:64001-64014.
38. Gao X, Sun L, Zhang N, Li C, Zhang J, Xiao Z, et al. Gestational Zearalenone Exposure Causes Reproductive and Developmental Toxicity in Pregnant Rats and Female Offspring. Toxins. 2017;9:21.
39. Wang D, Zhang N, Peng Y, Qi, D. Interaction of zearalenone and soybean isoflavone on the development of reproductive organs, reproductive hormones and estrogen receptor expression in prepubertal gilts. Anim. Reprod Sci. 2010;122:317-323.
40. Xu D, He H, Jiang X, Hua R, Chen H, Yang L, et al. Sirt2 plays a novel role on progesterone, estradiol and testosterone synthesis via PPARs/LXRα pathway in bovine ovarian granular cells. J. Steroid. Biochem. 2018;185:27-28.
41. Wang P, Liu S, Zhu C, Duan Q, Jiang Y, Gao K, et al. MiR-29 regulates the function of goat granulosa cell by targeting PTX3 via the PI3K/Akt/mTOR and Erk1/2 signaling pathways. J. Steroid. Biochem. 2020;202:105722.

Table

Table 1. Primers sequences were used for RT-PCR.

Genes	Primer sequences (5'–3')	Accession no.	Product size/bp
β-Actin	Forward: ATCAAGATCATCGCGCCTCC	XM-003124280.5	169
	Reverse: AATGCAACTAACAGTCCGCCT		
CYP19A1	Forward: TCCGCAATGACTTGGGCTAC	NM-21449.1	103
	Reverse: GCCTTTTCGTCCAGTGGGAT		
ER1	Forward: GCTACATCATCTCGCTTCCGT	NM-21220.1	115
	Reverse: ACTTCAGGGTGCTGGACAGA		
ER2	Forward: TCCTTTAGCCATCCATTGCC	XM-021081392.1	214
	Reverse: TCCTGACGCATAATCACTGCA		
FSHR	Forward: TTCACAGTCGCCCTCTTTCC	XM-021085884.1	152
	Reverse: CAGCCACAGATGACCACAAA		

Figures

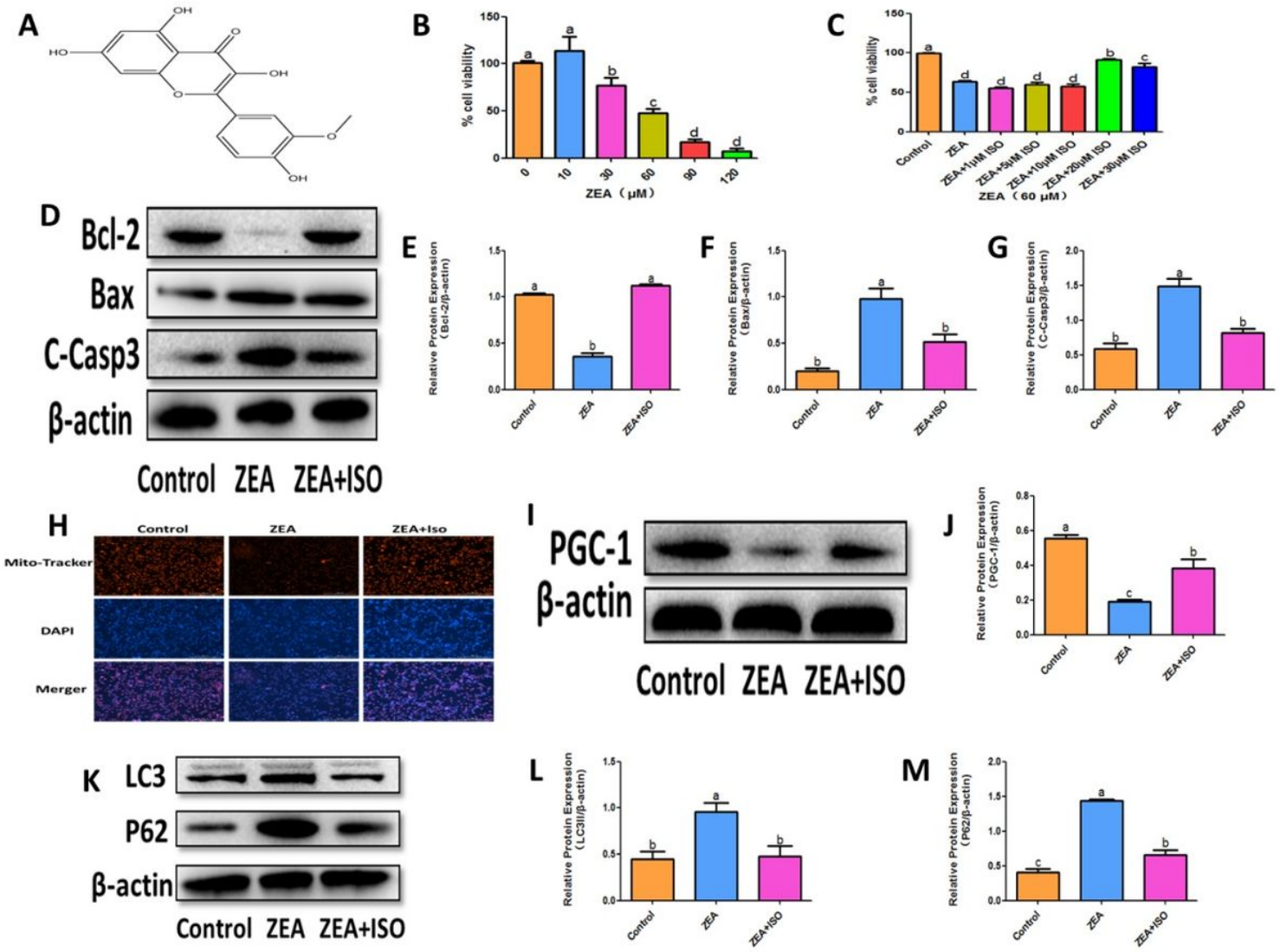

Figure 1

Isorhamnetin suppressed ZEA-induced apoptosis. GCs were cultured with isorhamnetin (20 μM) for 2 h, before treatment with ZEA (60 μM) for 24 h. (A) Structure of isorhamnetin. (B) The viability of GCs treated with ZEA for 24 h. (C) The effect of pretreatment with different concentrations of isorhamnetin on the viability of ZEA (60 μM)-exposed GCs. (D) WB shows of Bcl-2, Bax and C-Casp3 at various treatments. (E-G) The chart indicated the relative quantification of Bcl-2, Bax and C-Casp3 normalized to β-actin. (H) Representative images of mitochondrial distribution in the different groups. Scale bars = 200 μm. (I) WB analysis of PGC-1 in the different groups. (J) The bar graph showed the relative quantification of PGC-1 normalized to β-actin. (K) WB analysis of LC3 and P62 in the different groups. (L-M) The bar graph showed the relative quantification of LC3II and P62 normalized to β-actin. Data show means ± SEM. Different letters show significant differences ($P < 0.05$).

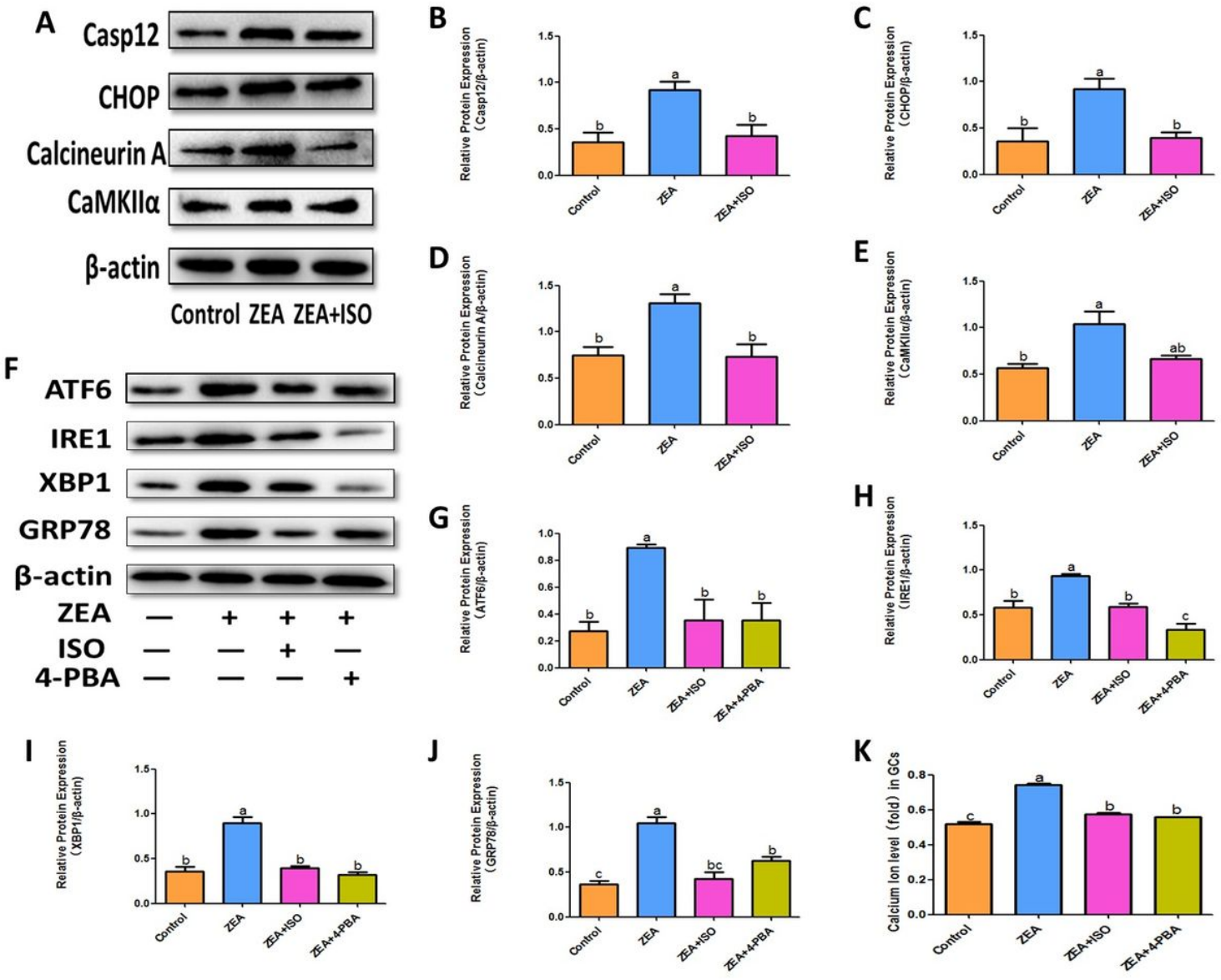

Figure 2

Isorhamnetin relieved ZEA-induced ERS. GCs were cultured with isorhamnetin (20 μM) for 2 h with or without 4-PBA (0.5 mM), before to ZEA treatment (60 μM) for 24 h. (A) WB analysis of Casp12, CHOP, CalcineurinA and CaMKIIα in at various treatments. (B-E) The bar chart represented the relative quantification of Casp12, CHOP, CalcineurinA and CaMKIIαin normalized to β-actin. (F) WB analysis of ATF6, IRE1, XBP1 and GRP78 at various treatments. (G-J)The bar chart represented the relative quantification of ATF6, IRE1, XBP1 and GRP78 normalized to β-actin. (K) Microplate reader analysis indicated intracellular Ca2+ levels at various treatments. Data show means ± SEM. Different letters show significant differences ($P < 0.05$).

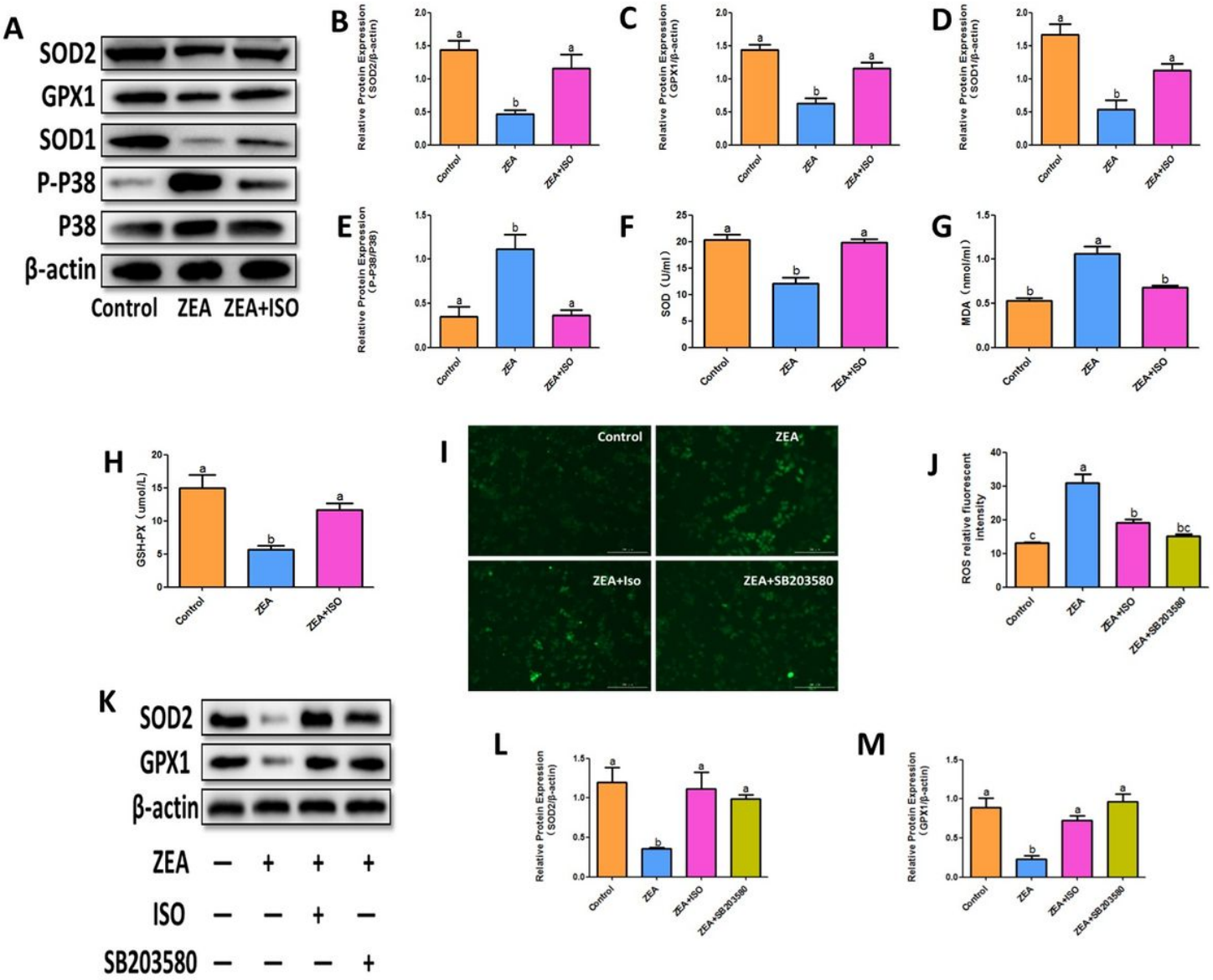

Figure 3

Isorhamnetin ameliorated ZEA-induced cytotoxicity by attenuating oxidative stress. GCs were cultured with isorhamnetin (20 μM) for 2 h with or without SB203580 (10 μM), prior to ZEA treatment (60 μM) for 24 h. (A) WB analysis of SOD2, GPX1, SOD1, P-P38 and P38 at various treatments. (B-E) The chart showed the relative quantification of SOD2/β-actin, GPX1/β-actin, SOD1/β-actin and P-P38/P38. (F-H) Levels of SOD, MDA and GSH-PX showed at various treatments. (I) The image showed the ROS. Scale bars = 200 μm. (J) The chart indcated the intracellular ROS at various treatments. (K) Protein expression levels of SOD2 and GPX1 at various treatments. (L-M) The bar chart represented the relative quantification of SOD2 and GPX1 normalized to β-actin. Data show means ± SEM. Different letters show significant differences ($P < 0.05$).

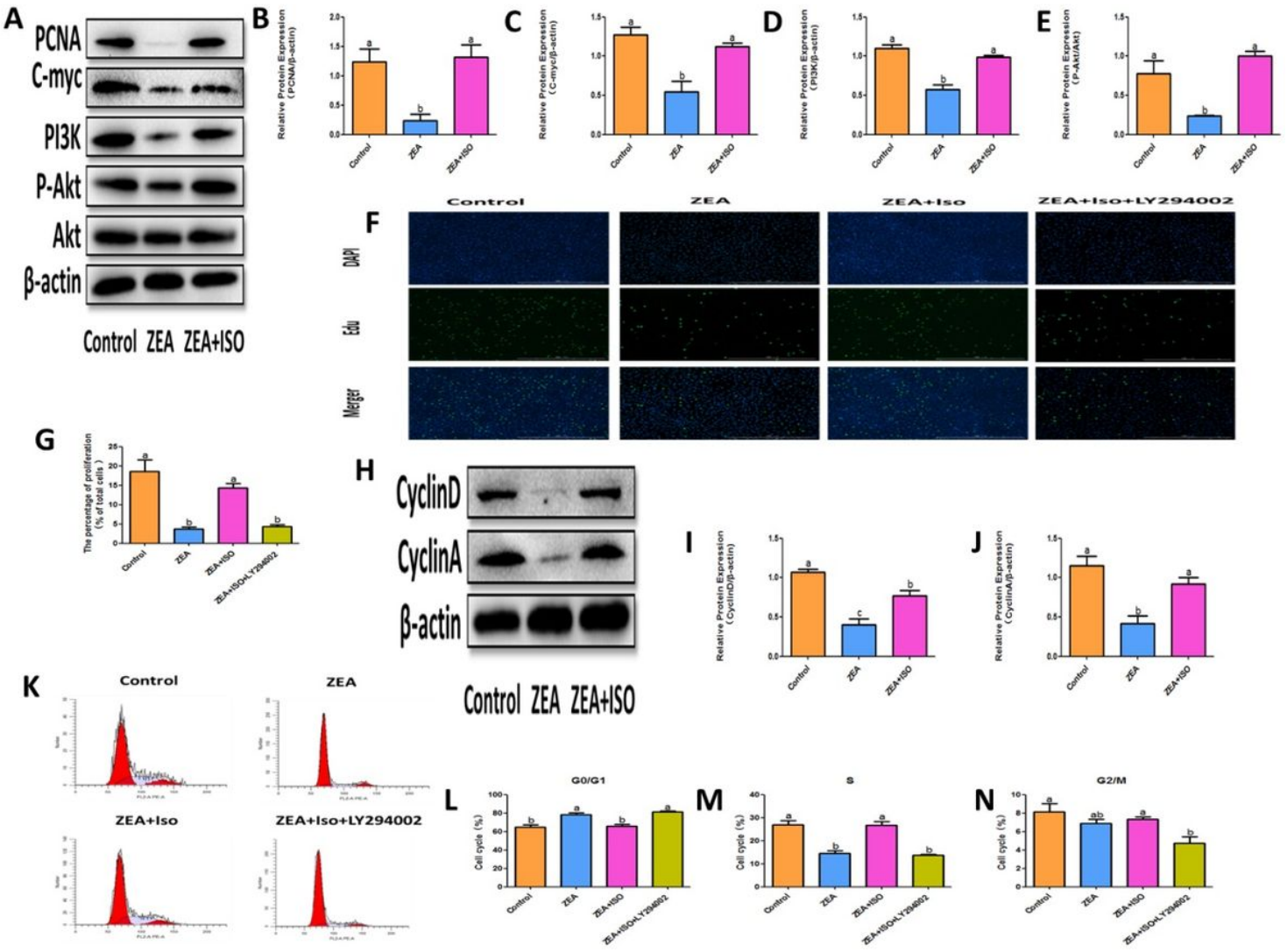

Figure 4

Isorhamnetin recovered GCs proliferation caused by ZEA. GCs were cultured with isorhamnetin (20 μM) for 2 h with or without LY294002 (20 μM), before treatment with ZEA (60 μM) for 24 h. (A) WB analysis of PCNA, C-myc, PI3K, P-Akt and Akt at various treatments. (B-E) The bar chart indicated the relative quantification of PCNA/β-actin, C-myc/β-actin, PI3K/β-actin, P-Akt/Akt, respectively. (F) GCs Image stained with EdU. Scale bars = 1,000 μm. (G) The bar chart represented the percentage of Edu-positive cell. (H) Western blot analysis of CyclinD and CyclinA at various treatments. (I-J) The bar chart showed the relative quantification of CyclinD and CyclinA normalized to β-actin. (K) Flow cytometry was detected the cell cycle. (L-N) The chart indicated the proportion of GCs in G1, S, G2 phase. Data show means ± SEM. Different letters show significant differences ($P < 0.05$).

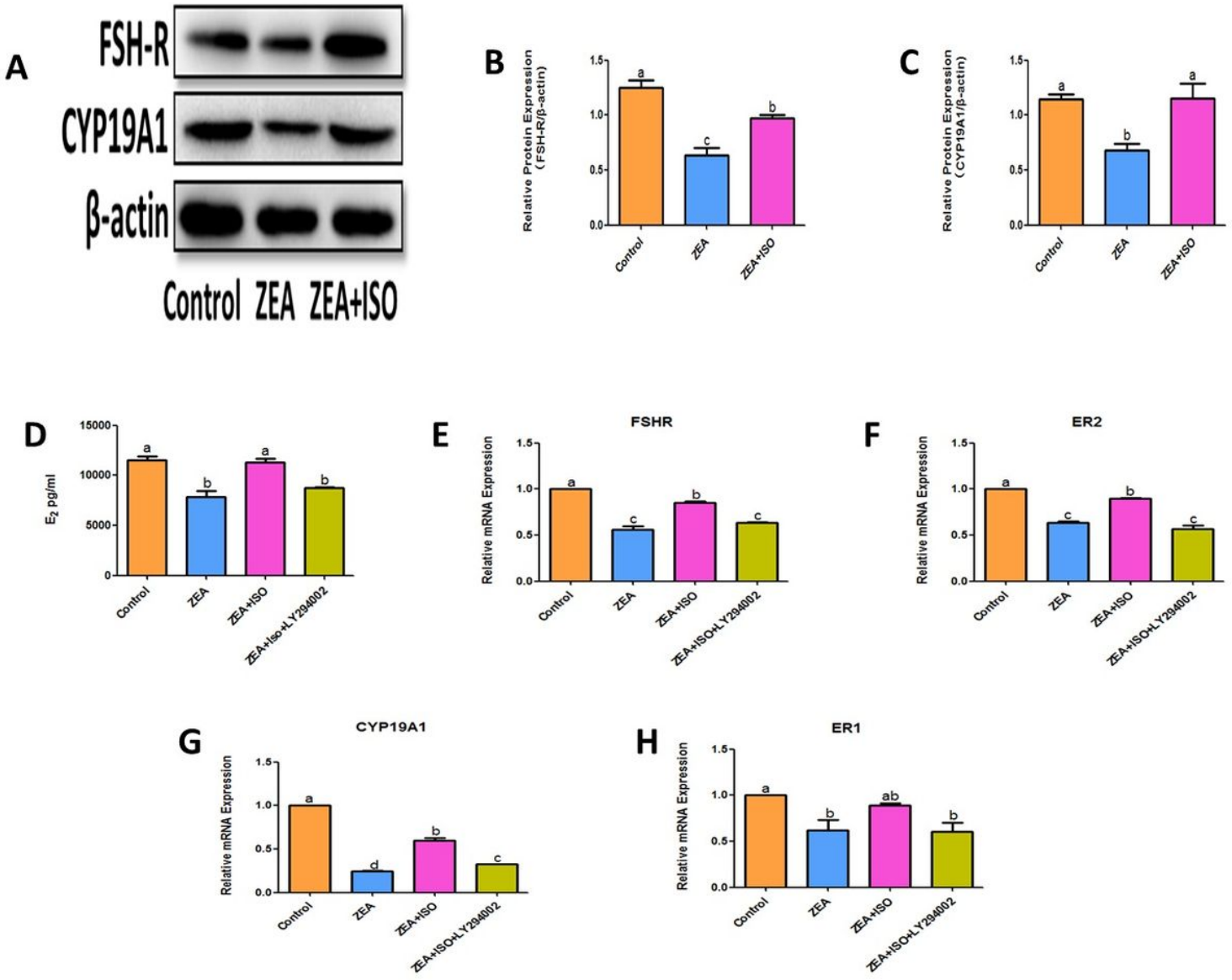

Figure 5

Isorhamnetin prevented ZEA-induced steroid secretion disorder in a PI3K/Akt-dependent manner. GCs were cultured with isorhamnetin (20 μM) for 2 h with or without LY294002 (20 μM), before treatment with ZEA (60 μM) for 24 h. (A) WB analysis of FSH-R and CYP19A1 at various treatments. (B-C) The bar chart showed the relative quantification of FSH-R and CYP19A1 normalized to β-actin. (D) The content of E2 in GCs. (E-H) The mRNA expression of FSH-R, ER2, CYP19A1 and ER1 were tested by an RT-PCR assay. Data show means ± SEM. Different letters show significant differences ($P < 0.05$).

Supplementary Files

This is a list of supplementary files associated with this preprint. Click to download.

- Graphic.jpg

- SupplementaryMaterial.docx